

## Supporting Information

### Construction of Frustrated Lewis Pairs on Carbon Nitride Nanosheet for Catalytic Hydrogenation of Acetylene

Qiang Wan<sup>a</sup>, Juan Li<sup>a</sup>, Rong Jiang<sup>b,\*</sup>, and Sen Lin<sup>a,c,\*</sup>

<sup>a</sup> *State Key Laboratory of Photocatalysis on Energy and Environment, College of  
Chemistry, Fuzhou University, Fuzhou 350002, China*

<sup>b</sup> *Institute of Advanced Energy Materials, Fuzhou University, Fuzhou 350002, China*

<sup>c</sup> *Fujian Provincial Key Laboratory of Theoretical and Computational Chemistry,  
Xiamen, Fujian 361005, China*

---

\*Corresponding author. Email: [slin@fzu.edu.cn](mailto:slin@fzu.edu.cn) (S.L)

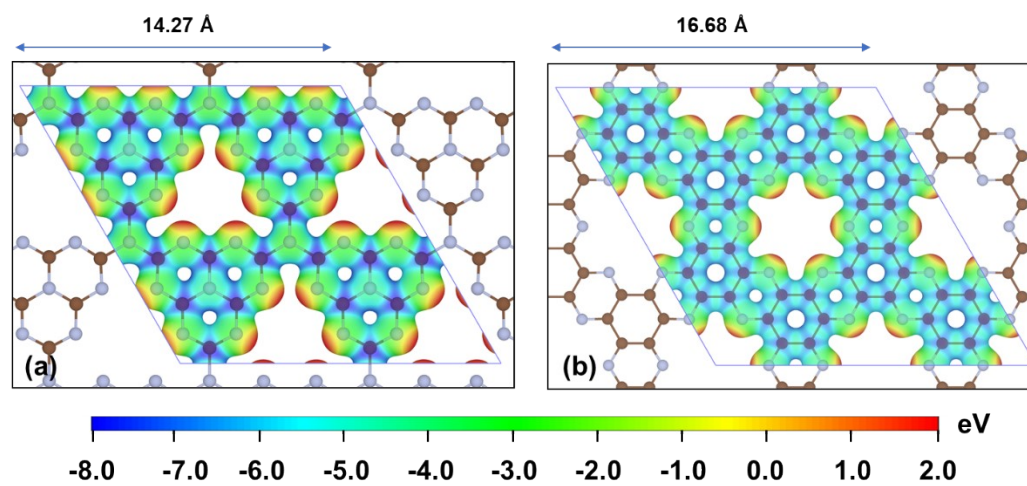


**Figure S1.** Optimized structures with charge density colored by local potential (eV) of (a)  $g\text{-C}_3\text{N}_4$  and (b)  $\text{C}_2\text{N}$ . Color code: C, brown; N, light blue. Isosurface level of charge density: 0.1 e bohr<sup>-3</sup>.

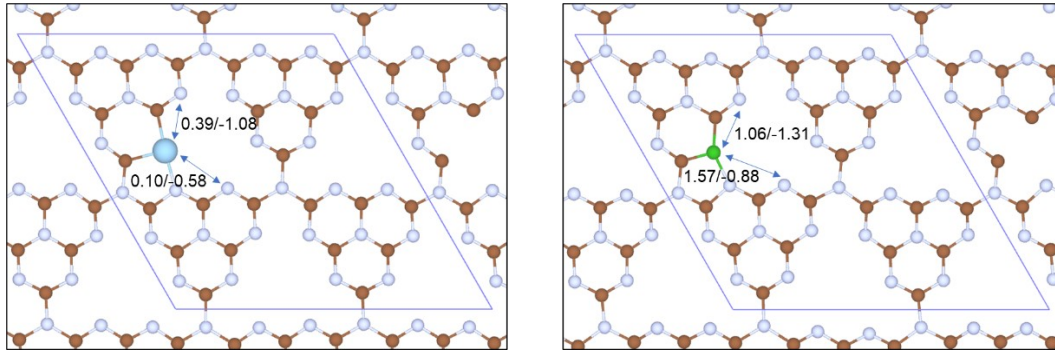


**Figure S2.** Comparison of H<sub>2</sub> dissociation on Al and B doped *g*-C<sub>3</sub>N<sub>4</sub>, with energy barrier/reaction energy.

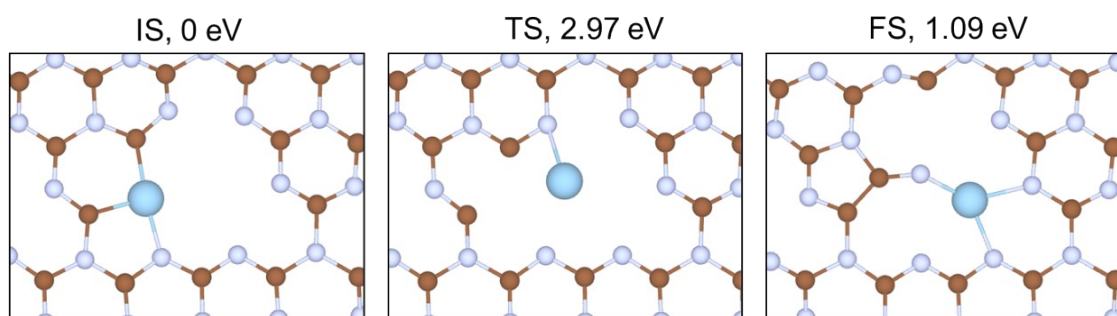


**Figure S3.** The initial, transition and final states of Al migration in the pore of the  $g$ - $C_3N_4$ , related energies are also attached.

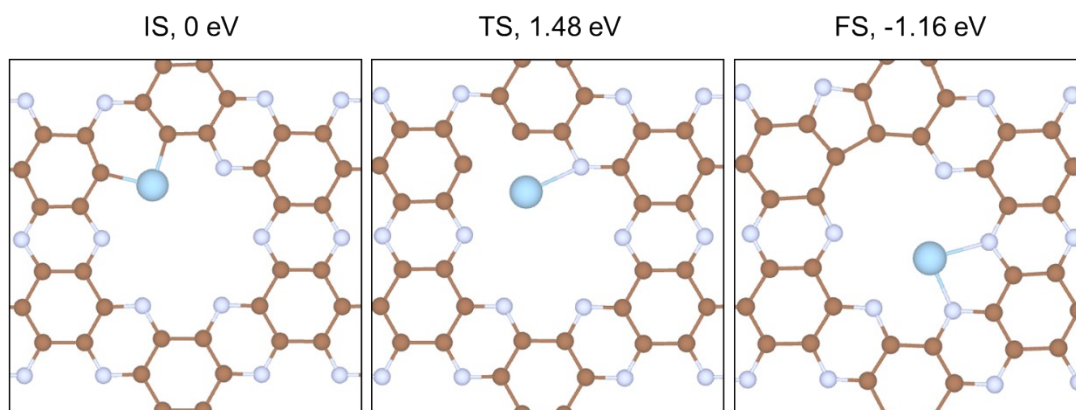


**Figure S4.** The initial, transition and final states of Al migration in the pore of the C<sub>2</sub>N, related energies are also attached.

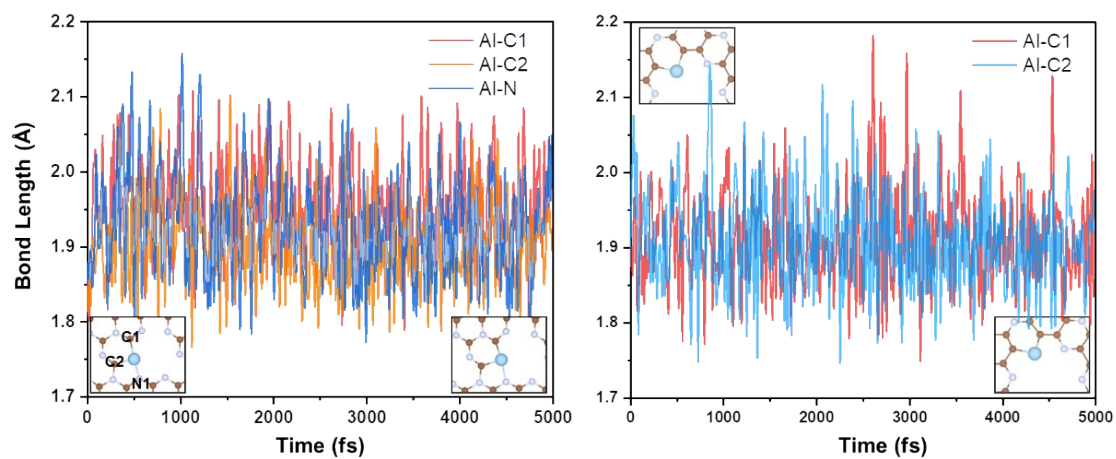


**Figure S5.** Bond length variation of Al–C/N bond in Al-doped  $g\text{-C}_3\text{N}_4$  (left) and  $\text{C}_2\text{N}$  (right) AIMD simulations under 500 K for 5ps.

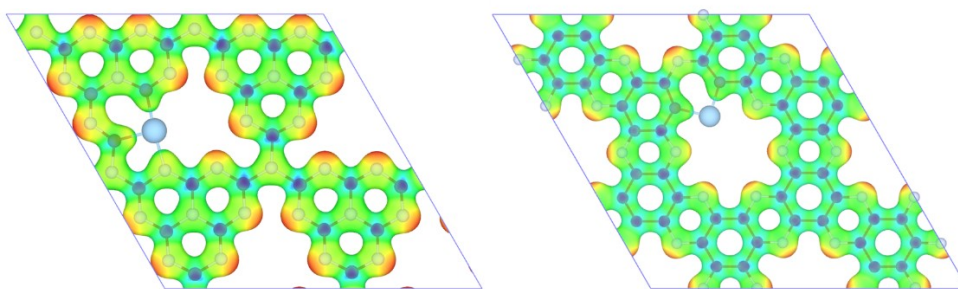


**Figure S6.** Electrostatic potential colored electron density Al doped  $g\text{-C}_3\text{N}_4$  and  $\text{C}_2\text{N}$ .

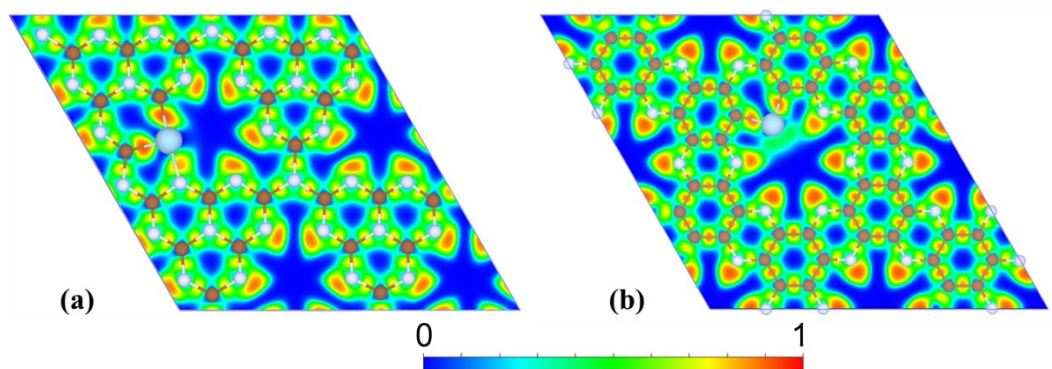


**Figure S7.** Electron localization function maps of Al-doped (a)  $g\text{-C}_3\text{N}_4$  and (b)  $\text{C}_2\text{N}$



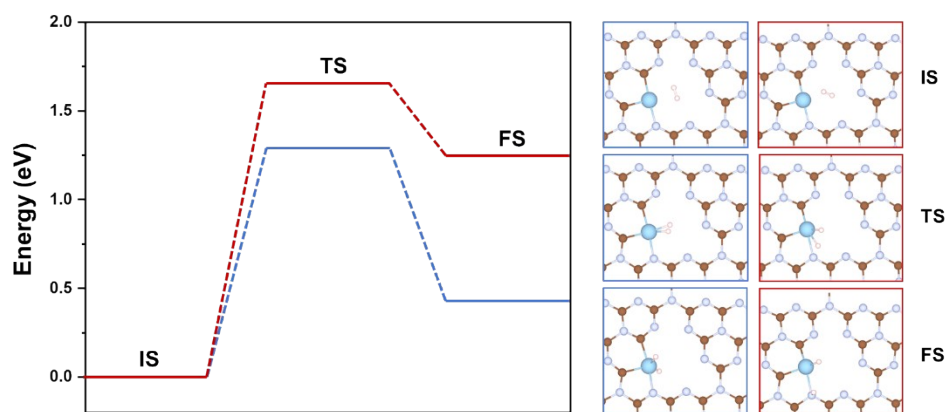


**Figure S8.** Comparison between the homolytic  $\text{H}_2$  dissociation on Al site (blue) and heterolytic  $\text{H}_2$  dissociation on CLP (red).

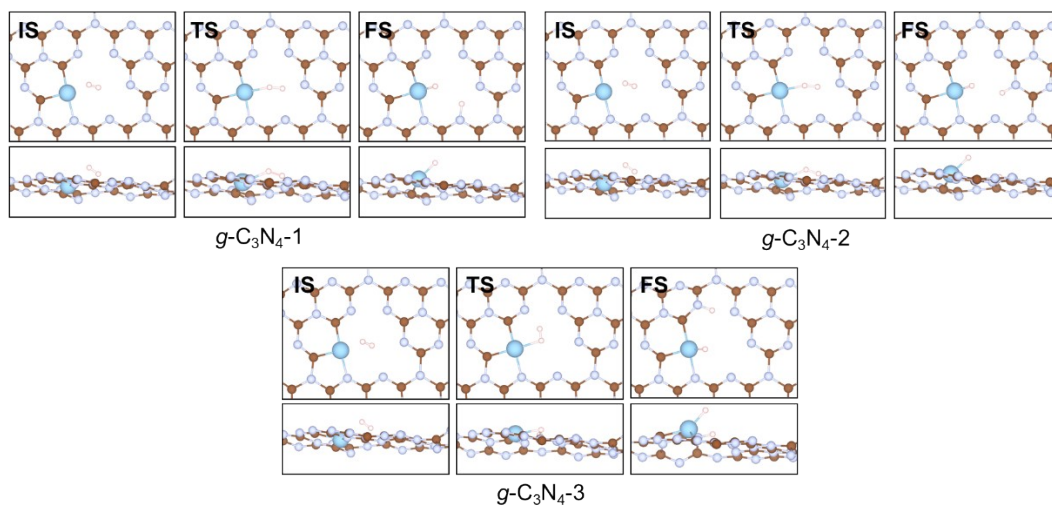


**Figure S9.** Initial (IS), transition (TS) and final states (TS) of  $\text{H}_2$  dissociation catalyzed by FLPs in Al-doped  $g\text{-C}_3\text{N}_4$ .

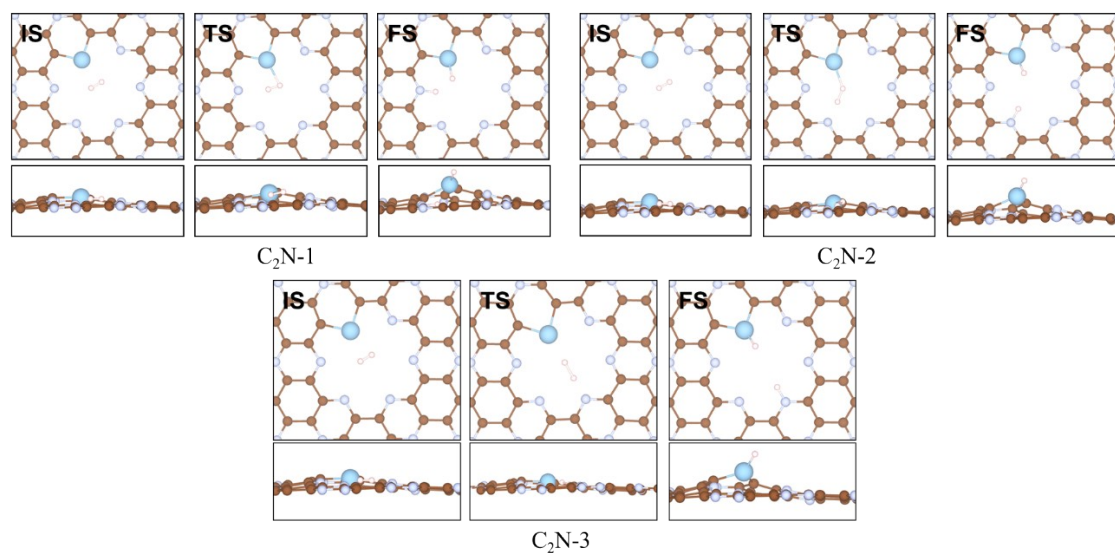


**Figure S10.** IS, TS and FS of H<sub>2</sub> dissociation catalyzed by FLPs in Al-doped C<sub>2</sub>N.

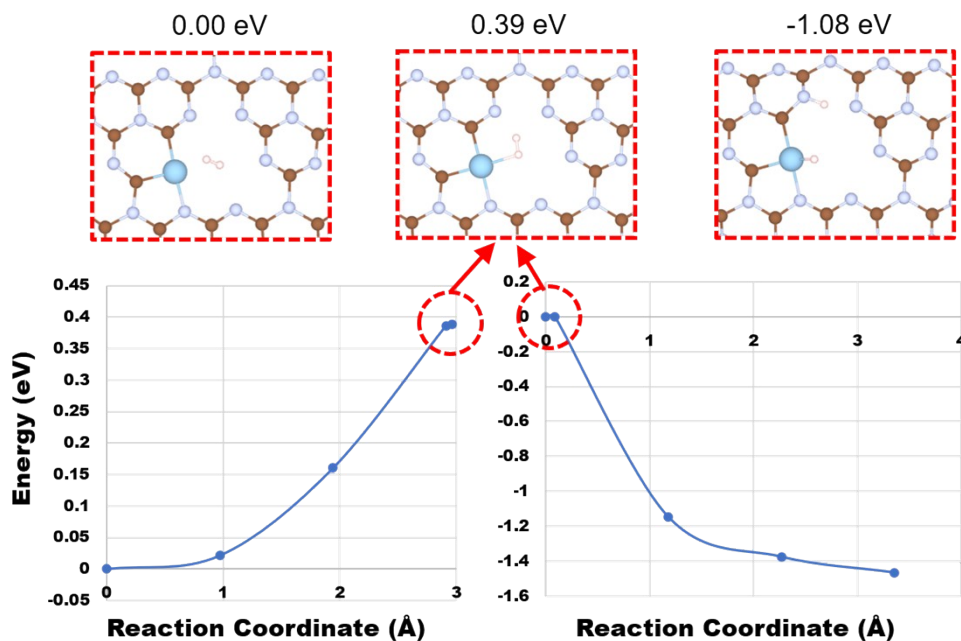


**Figure S11.** Reaction coordinate (split at metastable state) of  $\text{H}_2$  activation catalyzed by Al-doped  $g\text{-C}_3\text{N}_4\text{-3}$ , owing to the existence of a metastable state in the process.

Different from the other two FLPs, the pathway of  $\text{H}_2$  dissociation on  $g\text{-C}_3\text{N}_4\text{-3}$  involved a metastable state (MS,  $d_{\text{H-H}}=0.85 \text{ \AA}$ , without image frequency), which can be considered as an intermediate. To verify this path, we split the process into two steps, IS to MS and MS to FS, which can represent the orientation transformation of  $\text{H}_2$  and  $\text{H}_2$  cleavage, respectively. Results show that the former one is pure energetic climbing while the latter is downhill, both two steps would not experience a transition state. These suggest that starting from the same initial state with the other two FLPs, the  $\text{H}_2$  dissociation on  $g\text{-C}_3\text{N}_4\text{-3}$  should overcome an energy of 0.39 eV.

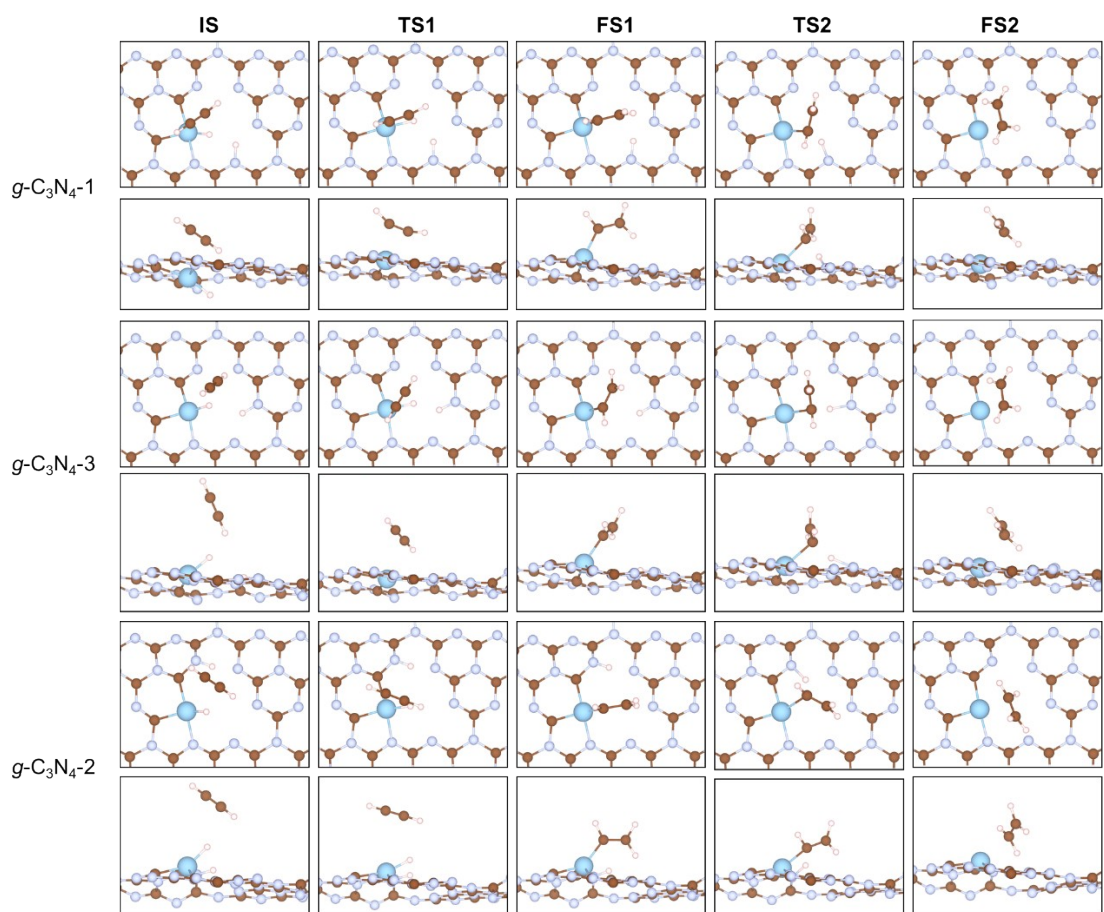


**Figure S12.** IS, TS and FS of acetylene hydrogenation catalyzed by FLPs in Al-doped  $g\text{-C}_3\text{N}_4$ .

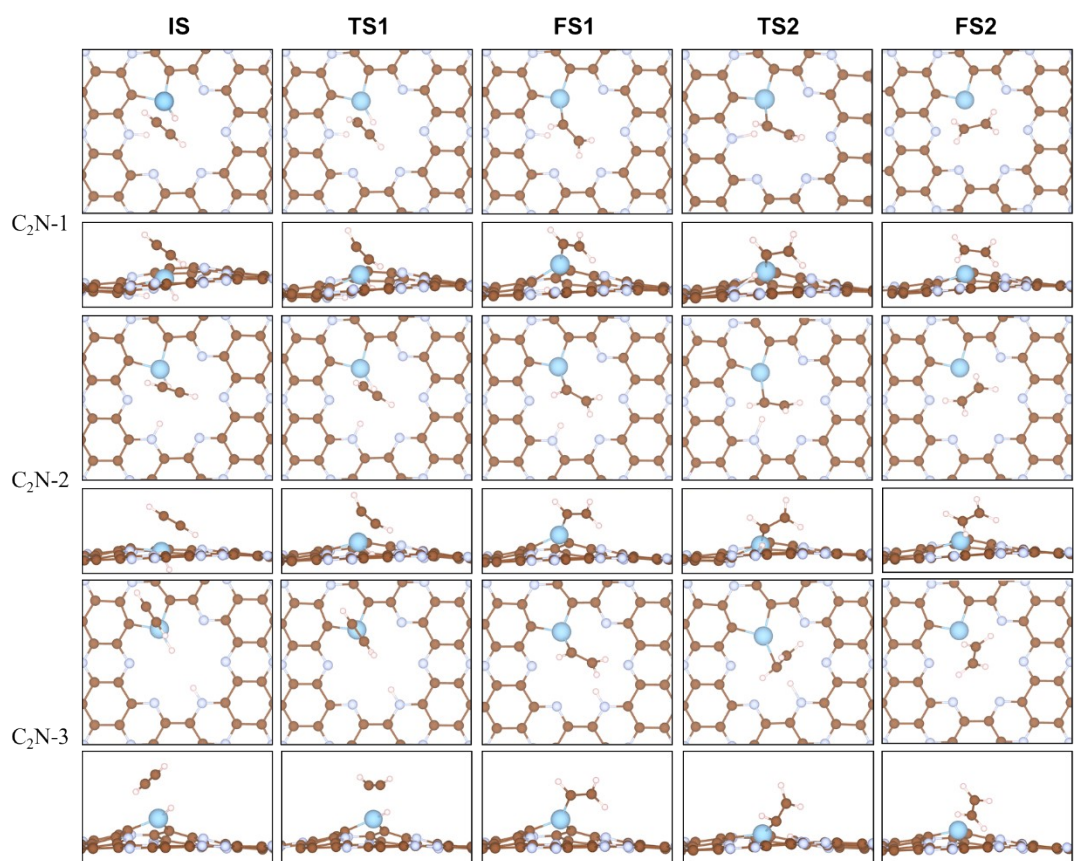


**Figure S13.** IS, TS and FS of acetylene hydrogenation catalyzed by FLPs in Al-doped  $C_2N$ .

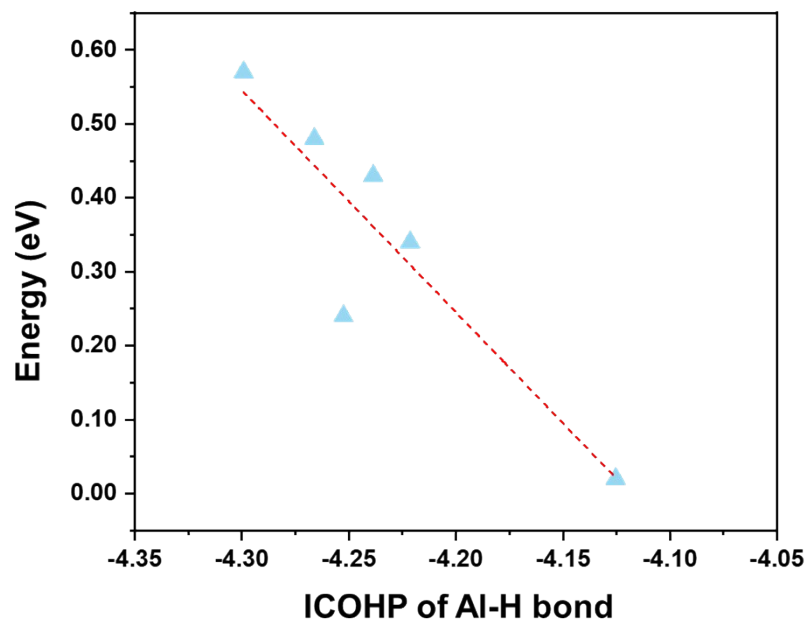


**Figure S14.** Correlation between the ICOHP of Al-H bond with the energy barrier of the first hydrogenation.

**Table S1.** Distance ( $d_{\text{N-LA}}$ ) of N-Al and adsorption energy ( $E_{\text{ads}}$ ) of LA for varying carbon nitride supporting LA. The cohesive energy of Al<sup>1</sup> and B<sup>2</sup> is 3.67 and 5.91 eV, respectively.

		Al		B	
		$d_{\text{N-LA}}$ (Å)	$E_{\text{ads}}$ (eV)	$d_{\text{N-LA}}$ (Å)	$E_{\text{ads}}$ (Å)
$g\text{-C}_3\text{N}_4$	adsorption	2.39-2.78	-2.86	2.67-3.52	-4.74
	substitution	3.29-4.16	-4.72	2.67-4.78	-10.92
$\text{C}_2\text{N}$	adsorption	2.87-3.61	-4.36	3.10-4.21	-5.17
	substitution	2.59-4.88	-4.18	2.87-5.60	-7.73



**Table S2.** Calculated distance between Al and N sites ( $d_{\text{Al-N}}$ ), atomic charge (Q) of hydrogen in transition state (TS), and H-H bond lengths ( $d_{\text{H-H}}$ ).

FLP sites	$d_{\text{Al-N}}/\text{\AA}$	$Q/e$ (TS)		$d_{\text{H-H}}/\text{\AA}$
		H(Al)	H(N)	
$g\text{-C}_3\text{N}_4\text{-1}$	3.29	-0.47	0.36	0.91
$g\text{-C}_3\text{N}_4\text{-2}$	4.16	-0.47	0.35	0.90
$g\text{-C}_3\text{N}_4\text{-3}$	3.68	-0.37	0.30	0.85
$\text{C}_2\text{N-1}$	2.59	-0.19	0.14	0.82
$\text{C}_2\text{N-2}$	4.26	-0.48	0.36	0.99
$\text{C}_2\text{N-3}$	4.28	-0.48	0.36	1.10

### References:

1. Sen, P.; Ciraci, S.; Buldum, A.; Batra, I. P., Structure of aluminum atomic chains. *Physical Review B* **2001**, *64* (19), 195420.
2. Hayami, W.; Otani, S., The Role of Surface Energy in the Growth of Boron Crystals. *The Journal of Physical Chemistry C* **2007**, *111* (2), 688-692.